Performance-Based Seismic Analysis of Light SDoF Secondary Substructures

Stavros Kasinos
PhD Candidate, School of Civil & Building Engineering, Loughborough University, UK

Alessandro Palmeri
Senior Lecturer, School of Civil & Building Engineering, Loughborough University, UK

Mariateresa Lombardo
Lecturer, School of Civil & Building Engineering, Loughborough University, UK

ABSTRACT: A novel procedure is presented for the application of the PBE (performance-based engineering) methodology to the seismic analysis and design of light secondary substructures. In the proposed technique, uncertainty is conveniently represented in the reduced modal subspace rather than geometric domain, which significantly reduces the number of uncertain parameters. The random response of a primary structure under earthquake excitation is investigated, various cases of linear and nonlinear secondary subsystems are examined and the propagation of uncertainty from the dynamic properties of the primary structure to the seismic performance of the secondary subsystems is quantified.

1. INTRODUCTION

Secondary subsystems are components or contents of buildings that do not form part of the primary load-bearing structure. Examples include architectural, mechanical and electrical components, building equipment or furniture, which can be modelled as single-degree-of-freedom (SDoF) oscillators or multi-degree-of-freedom (MDoF) structures, either linear or nonlinear, singly or multiply connected to the primary structure. Their seismic analysis and design is a topic of key engineering interest because their damage can cause injuries or deaths, as well as interruption of services, which in turn can lead to further human and economic losses (e.g. Taghavi and Miranda, 2003) .

The primary focus in earthquake engineering has historically been on structural resistance, providing designers with guidance to ensure life safety. This has mainly been addressed by specifying prescriptive and inexplicit requirements, e.g. limiting stresses and deformations determined from nominal design loads. Aimed at enabling a more predictable performance, as well as allowing different targets to be achieved for building structures in dialogue with the relevant stakeholders, performance-based engineering (PBE) philosophy has recently emerged as a broad spectrum of design solutions underpinned by well-defined case-specific performance objectives.

Inherent uncertainties in the specification of ground shaking and structural properties (e.g. strength and stiffness of members and connections) induce variation in the seismic performance of structures. While these uncertainties are implicitly considered within a prescriptive design (i.e. through partial safety factors and characteristic values), PBE allows a rational estimation of their effects in a probabilistic manner.

The implementation of PBE for secondary substructures is limited within the technical literature. Goulet et al. (2007) demonstrated the application of the methodology to reinforced-concrete moment-resisting frames, highlighting the impact of key modelling assumptions on the accurate calculation of damage and associated repair costs. Yang et al. (2007) adopted a full probabilistic implementation of PBE for the performance evaluation of facilities, in which nonstructural components were classified into performance groups based on their sensitivity to engineering demand parameters (EDPs).

In this paper, a simulation-based procedure is presented for the application of the PBE methodology to the seismic analysis of light subsystems. Rather than being directly defined in the geometric (physical) domain, in the proposed approach, uncertainty is characterised in the modal subspace, with modal shapes, modal frequencies and damping ratios constituting the random quantities, which noticeably reduces the number of uncertain parameters and the size of the dynamic problem. Both linear and nonlinear SDoF oscillators (attached to a linear MDoF system) are considered, as representatives of a wider spectrum of nonstructural components, and the propagation of uncertainty from the primary structure to the secondary subsystems is quantified.

2. GOVERNING EQUATIONS

If the secondary system is assumed to be "light" (e.g. Muscolino and Palmeri, 2007), i.e. the secondary attachment's mass m_S is much less than the mass of the primary structure M_P ($m_\mathrm{S} \ll M_\mathrm{P}$), a cascade-type approach is admissible, with the two systems being decoupled and sequentially analysed. Initially, the seismic response of the primary system is evaluated neglecting the feedback of the secondary, with the response of the secondary successively being computed at the points of attachment. In this approach no primary-secondary interaction is taken into account.

2.1. Linear primary system

Let us consider the case of a MDoF primary system. Within the linear-elastic range, its seismic motion is ruled by:

$$\mathbf{M} \cdot \ddot{\mathbf{u}}(t) + \mathbf{C} \cdot \dot{\mathbf{u}}(t) + \mathbf{K} \cdot \mathbf{u}(t) = -\mathbf{M} \cdot \boldsymbol{\tau} \cdot \ddot{u}_g(t), \quad (1)$$

where $\mathbf{M}$, $\mathbf{C}$ and $\mathbf{K}$ are matrices of mass, equivalent viscous damping and elastic stiffness, respectively; $\mathbf{u}(t)$ is the array collecting the degrees of freedom (DoFs) of the system; $\boldsymbol{\tau}$ is a vector of seismic incidence; $\ddot{u}_g(t)$ is the ground acceleration.

The equations of motion can be projected to the modal space, reducing the size of the dynamic problem from n (system's DoFs) to m (the number of modes retained within the analysis). This requires solving the real-valued eigenproblem:

$$\mathbf{M} \cdot \boldsymbol{\Phi} \cdot \boldsymbol{\Omega}^2 = \mathbf{K} \cdot \boldsymbol{\Phi}, \quad (2)$$

where $\boldsymbol{\Phi}$ is the normalized modal matrix and $\boldsymbol{\Omega}$ the diagonal spectral matrix.

It has been shown (Palmeri and Lombardo, 2011) that the truncation error introduced by the reduced modes can be corrected via a dynamic mode acceleration method (DyMAM). Accordingly, the dynamic response can be expressed as the sum of modal contributions and a corrective term:

$$\mathbf{u}(t) = \boldsymbol{\Phi} \cdot \mathbf{q}(t) + \Delta\mathbf{b}\,\omega_f^2\,\theta(t), \quad (3)$$

where $\mathbf{q}(t)$ is the array collecting the modal coordinates, ruled by the equation of motion in the modal space:

$$\ddot{\mathbf{q}}(t) + 2\,\zeta\,\boldsymbol{\Omega} \cdot \dot{\mathbf{q}}(t) + \boldsymbol{\Omega}^2 \cdot \mathbf{q}(t) = \mathbf{p} \cdot \ddot{\mathbf{u}}_\mathbf{g}(t), \quad (4)$$

in which:

$$\mathbf{p} = -\boldsymbol{\Phi}^\top \cdot \mathbf{M} \cdot \boldsymbol{\tau}, \quad (5)$$

while $\Delta\mathbf{b}$ is the static correction vector and $\theta(t)$ is the response of the oscillator satisfying:

$$\ddot{\theta}(t) + 2\,\zeta_f\,\omega_f\,\dot{\theta}(t) + \omega_f^2\,\theta(t) = \ddot{u}_g(t), \quad (6)$$

in which ω_f and ζ_f are chosen as:

$$\omega_f = 2\min\{\boldsymbol{\Omega}\}\ ; \quad \zeta_\mathrm{f} = \frac{1}{\sqrt{2}}. \quad (7)$$

2.2. Uncertainty in the modal subspace

In the preceding subsection, the analysis procedure to calculate the deterministic response of the primary structure was described, in which the equations of motion are conveniently projected to the reduced modal subspace, reducing the size of the dynamic problem (Falsone and Muscolino, 2004). Likewise, efficient analysis methods of combined primary-secondary systems (Biondi and Muscolino, 2000) utilise modal analysis to predict the dynamic interaction between the two components. In accordance with the PBE philosophy, the probabilistic response is of interest, whereby uncertainty consideration needs to be explicit (FIB, 2012). Contrary to the existing methods where uncertainty is treated in the full nodal space, the present study, is motivated by the need to characterise uncertainty in the reduced modal domain significantly reducing the number of uncertain parameters. This can be achieved by considering some random fluctuations in the eigenvectors, such that the stochastic modal matrix will read:

$$\hat{\mathbf{\Phi}} = \begin{bmatrix} \boldsymbol{\phi}_1^\top + \alpha_{1,2}\boldsymbol{\phi}_2^\top + \alpha_{1,3}\boldsymbol{\phi}_3^\top + \cdots + \alpha_{1,m}\boldsymbol{\phi}_m^\top \\ \alpha_{2,1}\boldsymbol{\phi}_1^\top + \boldsymbol{\phi}_2^\top + \alpha_{2,3}\boldsymbol{\phi}_3^\top + \cdots + \alpha_{2,m}\boldsymbol{\phi}_m^\top \\ \vdots \\ \alpha_{m,1}\boldsymbol{\phi}_1^\top + \alpha_{m,2}\boldsymbol{\phi}_2^\top + \alpha_{m,3}\boldsymbol{\phi}_3^\top + \cdots + \boldsymbol{\phi}_m^\top \end{bmatrix}^\top, \tag{8}$$

$\boldsymbol{\phi}$ being a modal shape, and α an independent random coefficient for each mode.

It can be shown that by modifying the deterministic Eq. (4) in light of Eq. (8), and applying similar considerations to the modal frequencies and the energy dissipation, the stochastic solution of the system will be governed by a differential equation of the form:

$$\hat{\mathbf{m}} \cdot \ddot{\hat{\mathbf{q}}}(t) + \hat{\mathbf{c}} \cdot \dot{\hat{\mathbf{q}}}(t) + \hat{\mathbf{k}} \cdot \hat{\mathbf{q}}(t) = \hat{\mathbf{p}} \cdot \ddot{u}_g(t), \tag{9}$$

where $\hat{\mathbf{m}}$, $\hat{\mathbf{c}}$ and $\hat{\mathbf{k}}$ represent the stochastic mass, damping and stiffness matrices in the reduced modal space respectively, such that:

$$\hat{\mathbf{m}} = \mathbf{I_m} + \boldsymbol{\alpha} + \boldsymbol{\alpha}^\top; \tag{10}$$

$$\hat{\mathbf{c}} = 2\zeta\left([\mathbf{I_m} + \boldsymbol{\alpha} + \boldsymbol{\beta}]\,\mathbf{\Omega} + \mathbf{\Omega}\,[\boldsymbol{\alpha} + \boldsymbol{\gamma}]^\top\right); \tag{11}$$

$$\hat{\mathbf{k}} = [\mathbf{I_m} + \boldsymbol{\alpha} + \boldsymbol{\beta}]\,\mathbf{\Omega}^2 + \mathbf{\Omega}^2\,[\boldsymbol{\alpha} + \boldsymbol{\beta}]^\top, \tag{12}$$

while $\hat{\mathbf{q}}(t)$ is the array collecting the random response and $\hat{\mathbf{p}}$ the seismic incidence vector:

$$\hat{\mathbf{p}} = \left[\mathbf{I_m} + \boldsymbol{\alpha} + \boldsymbol{\alpha}^\top\right]\mathbf{p}. \tag{13}$$

It is worth emphasising here that, in the proposed formulation, three sources of uncertainty are considered, namely the mass (through the modal shapes), modal frequencies and viscous damping ratios, respectively, each associated with a zero mean random matrix, namely, $\boldsymbol{\alpha}$, $\boldsymbol{\beta}$ and $\boldsymbol{\gamma}$, such that:

$$\boldsymbol{\alpha} = \begin{bmatrix} 0 & \alpha_{1,2} & \dots & \alpha_{1,m} \\ \alpha_{2,1} & 0 & \dots & \alpha_{2,m} \\ \vdots & \vdots & \ddots & \vdots \\ \alpha_{m,1} & \alpha_{m,2} & \dots & 0 \end{bmatrix}; \tag{14}$$

$$\boldsymbol{\beta} = \begin{bmatrix} \beta_1 & & \\ & \ddots & \\ & & \beta_m \end{bmatrix}; \boldsymbol{\gamma} = \begin{bmatrix} \gamma_1 & & \\ & \ddots & \\ & & \gamma_m \end{bmatrix}, \tag{15}$$

giving rise to a total of $m^2 + m$ statistically independent random coefficients.

2.2.1. *Verification*

It is possible to confirm the validity of the aforementioned formulation for a SDoF case ($m = 1$) by evaluating the stochastic quantities $\hat{\omega}$ and $\hat{\zeta}$. Particularising Eqs. (10) to (12), imposing a Taylor expansion about $\alpha, \beta, \gamma = 0$, and dropping high order terms, one gets:

$$\begin{aligned} \hat{\omega} &= \sqrt{\frac{\hat{k}}{\hat{m}}} = \omega \cdot \sqrt{\frac{1 + 2\alpha + 2\beta}{1 + 2\alpha}} \\ &\cong \omega \cdot \left(1 + \beta - 2\alpha\beta - \frac{\beta^2}{2} + \dots\right) \cong \omega\,(1 + \beta) \end{aligned} \tag{16}$$

and:

$$\begin{aligned} \hat{\zeta} &= \frac{\hat{c}}{2\hat{\omega}\hat{m}} = \zeta \frac{1 + 2\alpha + \beta + \gamma}{1 + 2\alpha + \beta + 2\alpha\beta} \\ &= \zeta\,(1 + \gamma - 2\alpha\beta - 2\alpha\gamma - \beta\gamma + \dots) \\ &\cong \zeta\,(1 + \gamma)\,. \end{aligned} \tag{17}$$

It follows that the standard deviation of the dimensionless random variables α, β and γ is the coefficient of variation (CoV) of the associated physical quantity.

2.3. *Nonlinear secondary oscillator*

Both linear and nonlinear SDoF oscillators have been considered as secondary subsystems. In the first case the equation of motion reads:

$$\ddot{u}_{\mathrm{s}}(t) + 2\,\zeta_{\mathrm{s}}\,\omega_{\mathrm{s}}\,\dot{u}_{\mathrm{s}}(t) + \omega_{\mathrm{s}}^2\,u_{\mathrm{s}}(t) = -\ddot{u}_{\mathrm{p}}^{(\mathrm{a})}(t), \tag{18}$$

where $\ddot{u}_{\mathrm{p}}^{(\mathrm{a})}(t) = \ddot{u}_{\mathrm{p}}(t) + \ddot{u}_{\mathrm{g}}(t)$ is the absolute acceleration of the primary structure at the position where the secondary system is attached.

For the nonlinear case, the governing equation can be posed in the form:

$$\ddot{u}_{\mathrm{s}}(t) + \frac{1}{m_{\mathrm{s}}}\,f_{\mathrm{s,nonlin}}(t) = -\ddot{u}_{\mathrm{p}}^{(\mathrm{a})}(t), \tag{19}$$

in which $f_{\mathrm{s,nonlin}}(t)$ is the nonlinear restoring force in the secondary SDoF oscillator, whose mathematical definition depends on the particular type of nonlinear behaviour.

For an elastic-perfectly plastic secondary subsystem, the evolution in time of the restoring force is ruled by:

$$\dot{f}_{\mathrm{s,nonlin}}(t) = \begin{cases} K_{\mathrm{s}}\,\dot{u}_{\mathrm{s}}(t) \\ \quad \text{if } |f_{\mathrm{s,EPP}}(t)| < f_{\mathrm{s,y}} \\ \quad \text{or } |f_{\mathrm{s,EPP}}(t)| = f_{\mathrm{s,y}} \text{ and} \\ \qquad f_{\mathrm{s,EPP}}(t)\,\dot{u}_{\mathrm{s}}(t) < 0\,; \\ \\ 0 \\ \quad \text{otherwise,} \end{cases} \tag{20}$$

in which $f_{\mathrm{s,y}}$ is the yielding force in the secondary oscillator.

The case of a rigid-perfectly plastic SDoF system can be considered as the limiting case of the above restoring force, when $K_{\mathrm{s}} \to +\infty$. As a result, the equation of motion becomes:

$$\ddot{u}_{\mathrm{s}}(t) = \begin{cases} -\ddot{u}_{\mathrm{p}}^{(\mathrm{a})}(t) + \mu_{\mathrm{s}}\,g\,\mathrm{sgn}\left(\ddot{u}_{\mathrm{p}}^{(\mathrm{a})}(t)\right) \\ \qquad \text{if } \left|\ddot{u}_{\mathrm{p}}^{(\mathrm{a})}(t)\right| > \mu_{\mathrm{s}}\,g\,; \\ \\ 0 \\ \qquad \text{otherwise,} \end{cases} \tag{21}$$

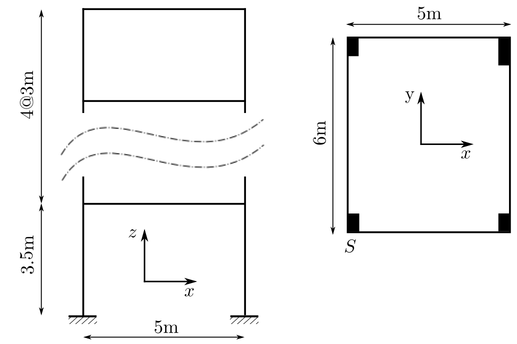

Figure 1: Structural frame model.

in which μ_{s} is the friction coefficient for the secondary system and g is the acceleration due to gravity.

3. NUMERICAL APPLICATION

The proposed formulation has been applied for the analysis of two subsystems in cascade.

Fig. 1 shows a MDoF primary system comprising of a 5-storey single-bay moment-resisting frame, being irregular in plan, with position S denoting the point of attachment of a light secondary SDoF oscillator of unit mass, modelled as (i) linear, (ii) elastoplastic and (iii) rigid-plastic. Floors are rigid in plane, while the self-weight and super-dead load constitute the mass source of the structure. The fundamental period of vibration is T_p=0.498s for the primary, and 0.9T_p for the secondary (cases (i) and (ii)). The total number of DoFs is n=15, with only m=6 retained in the analysis, chosen such that at least 90% of the modal mass participates in the seismic motion, a criterion set by current codes of practice (e.g. Eurocode 8, 2004).

A range of recorded accelerograms are applied in the x direction, chosen as representative of various scenarios (Cecini and Palmeri, 2015), namely El Centro 1940, Erzincan 1992 and Irpinia 1980, with peak ground accelerations (PGAs) of 0.313g, 0.515g and 0.177g, respectively.

3.1. *Uncertainty characterisation*

Uncertainty in the mass, modal frequencies and viscous damping ratios of the primary system is represented and propagated to the secondary system, with CoVs chosen as 0.025, 0.05 and 0.15 respectively, for two separate assumed distributions namely, uniform and Gaussian.

Although extendible to other methods, the results are presented only for a Monte-Carlo simulation (MCS), which is used to generate the randomised matrices, with a number of realisations $n_{\text{sym}} = 1,000$.

3.2. *Performance measures*

To quantify the response statistics and assess the propagation of uncertainty from the primary to the secondary subsystem, different performance measures (PMs) are defined. It is acknowledged that, various components are sensitive to different structural response parameters and thus PMs are chosen as: the maximum absolute acceleration and relative displacement respectively, for both linear primary and secondary systems; the total accumulated plastic deformation for the elastoplastic nonlinear; and maximum sliding distance for the rigid plastic.

3.3. *Primary system response*

A selection of results for the primary system is presented in this section. In a first stage, the frequency response function (FRF) has been evaluated for the primary system. Fig. 2(a) shows the exact FRF in the geometric space, by retaining all modes (m=n); by using the mode displacement method (MDM), with m=6, where no correction is applied; by using the MAM and DyMAM, which introduce a static and dynamic correction, respectively. It is evident that, while MAM produces an error in the high frequency range, this is seen to be corrected by DyMAM, which gives an improved approximation and is thus exploited in the subsequent stages.

Fig. 2(b) compares the exact deterministic response (black line) with the 1,000 realisations obtained with the proposed randomisation of the modal information, also corrected by DyMAM, for the case of uniform distribution (light grey), and Gaussian distribution (grey). For both cases, the proposed randomisation seems to be satisfactory in the frequency domain, with a higher fluctuation caused by the Gaussian distribution attributed to its unbounded nature.

Carrying out the dynamic analysis in the time domain (Fig. 3), one can observe that the oscillations of the randomised response tend to show significant fluctuations around the deterministic ones, with the uncertainty propagating with time, in all acceleration and displacement time histories.

Fig. 4 quantifies the statistics of the two PMs of the primary system under Irpinia ground motion record and Gaussian distribution, with μ, σ and CoV denoting mean, standard deviation and coefficient of variation of the stochastic output, and x being the deterministic (reported as a reference value).

Notably, the output CoV shows a 47% increase from acceleration (CoV=0.09) to displacement (CoV=0.132), suggesting that the choice of the PM is significant. Furthermore, both CoVs exceed the assumed input CoVs for mass and frequency (0.025, 0.05 respectively), while displacement PM lies close to the chosen input CoV for damping.

3.4. *Secondary system response*

Following the seismic response of the primary structure, our analyses proceed with the cascade response of three secondary oscillators. Fig. 5 compares the stochastic and deterministic force (top) and displacement (bottom) time histories for the linear (left), elastoplastic (middle) and rigid plastic (right) secondary systems, respectively.

In all three cases, as expected, the proposed randomisation seems satisfactory, with the time histories of the PMs fluctuating around the deterministic response.

Fig. 6 illustrates the normalised frequency distribution diagrams of the PM for the linear elastic, elastoplastic and rigid-plastic subsystems, respectively.

For the elastic case, the randomisation predicts a mean response of μ=0.179m, which is in good agreement with the deterministic value of x=0.182m. When compared to the corresponding relative displacement of the primary structure, an amplification of about 8 times is seen, which is attributed to resonance (the two systems being almost in-tune). The CoV=0.199 is higher than that of the primary system (0.132) as well as of the three sources of uncertainty of the input variables, suggesting that uncertainty has been amplified in the subsystem.

In the elastoplastic oscillator a value of x=0.723m in the corresponding PM shows that the

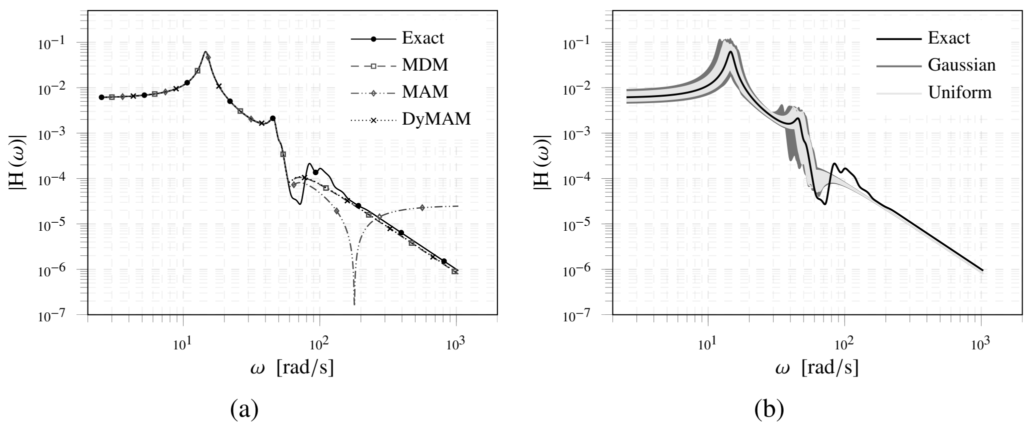

Figure 2: FRF for modal correction methods (a) and stochastic response (b).

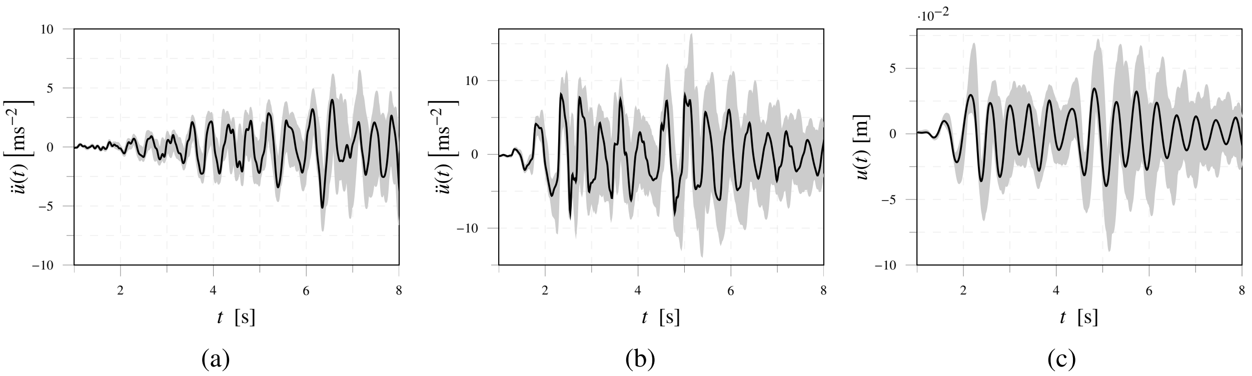

Figure 3: Acceleration time histories of Irpinia (left) and El Centro (middle); displacement time history of El Centro (right), drawn from Gaussian distributions.

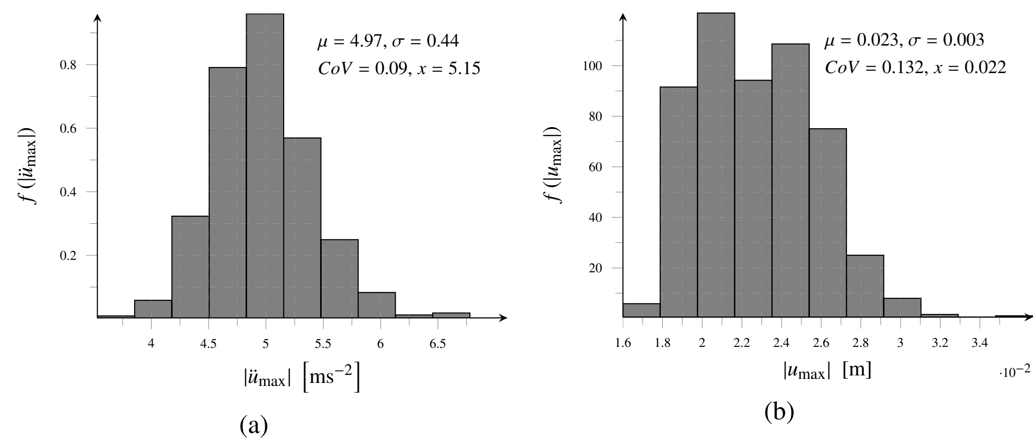

Figure 4: Frequency diagrams for acceleration (a) and displacement (b) primary system PMs for Irpinia earthquake, drawn from Gaussian distributions.

mean total plastic deformation is slightly underestimated (μ=0.746m), while a CoV=0.395, being much higher than the input parameters, suggests an increased dispersion in the results.

When the rigid-plastic oscillator is considered, a decrease of an order of magnitude in the corresponding PM is observed (when compared to the previous cases). Again, the resulting CoV of 0.279 is significantly higher than in the input, showing evidence of dispersion, which needs to be accounted for.

It therefore appears that, depending on the dynamic behaviour of the secondary system and its mechanical parameters, the seismic response can be significantly amplified, and the dispersion of results increased, meaning that a simple prescriptive approach to the design of such component can be under- or over- conservative.

4. CONCLUSIONS

A simulation-based procedure was presented for the application of the PBE methodology to the seismic analysis of light SDoF subsystems attached to a primary MDoF structure. A novel feature of the proposed approach is the characterisation of uncertainty in the reduced modal space, rather than in the full geometric domain, and its application in conjunction with a dynamic mode acceleration method (DyMAM). As demonstrated with Monte Carlo simulations, the proposed approach is capable of accurately representing the random dynamic response, despite the fact that the number of uncertain parameters is reduced to $m^2 + m$ statistically independent coefficients (m being the number of modes retained in analysis). The resulting model appears to be adequate for the purpose of assessing how uncertainty in the primary structure propagates to the seismic performance of the secondary subsystems.

In a first stage, the response of a primary structure subjected to different accelerograms was quantified through relevant performance measures (PMs), with uncertainty comprising the mass distribution, modal frequencies and damping. In a second stage, uncertainty in the primary system was propagated to i) linear, ii) elastoplastic and iii) rigid-plastic secondary systems, and the response statistics were quantified.

Future investigations will be carried out to assess the sensitivity of the output to the chosen random variation of the input parameters as well as their probabilistic distribution. The case of the rocking motion of a secondary subsystem will also be examined.

5. REFERENCES

Biondi, B. and Muscolino, G. (2000). "Component-mode synthesis method variants in the dynamics of coupled structures." *Meccanica*, 35(1), 17–38.

Cecini, D. and Palmeri, A. (2015). "Spectrum-compatible accelerograms with harmonic wavelets." *Computers and Structures*, 147, 26–35.

Eurocode 8 (2004). *European Commettee for Standardisation. Design of structures for earthquake resistance*.

Falsone, G. and Muscolino, G. (2004). "New real-value modal combination rules for non-classically damped structures." *Earthquake Engineering and Structural Dynamics*, 33, 1187–1209.

FIB (2012). *Probabilistic performance-based seismic design*. International Federation for Structural Concrete (fib), technical report, bulletin 68 Report, Lausanne, Switzerland.

Goulet, C. A., Haselton, C. B., Mitrani-Reiser, J., Beck, J. L., Deierlein, G. G., Porter, K. A., and Stewart, J. P. (2007). "Evaluation of the seismic performance of a code-conforming reinforced-concrete frame building – From seismic hazard to collapse safety and economic losses." *Earthquake Engineering and Structural Dynamics*, 36(13), 1973–1997.

Muscolino, G. and Palmeri, A. (2007). "An earthquake response spectrum method for linear light secondary substructures." *ISET Journal of Earthquake Technology*, 44(1), 193–211.

Palmeri, A. and Lombardo, M. (2011). "A new modal correction method for linear structures subjected to deterministic and random loadings." *Computers and Structures*, 89, 844–854.

Taghavi, S. and Miranda, E. (2003). *Response assessment of nonstructural building elements*. PEER Report 2003/05, University of California Berkeley.

Yang, T. Y., Moehle, J., Stojadinovic, B., and Kiureghian, A. D. (2007). "Seismic performance evaluation of facilities: Methodology and implementation." *Journal of Structural Engineering*, 135(10), 1146–1154.

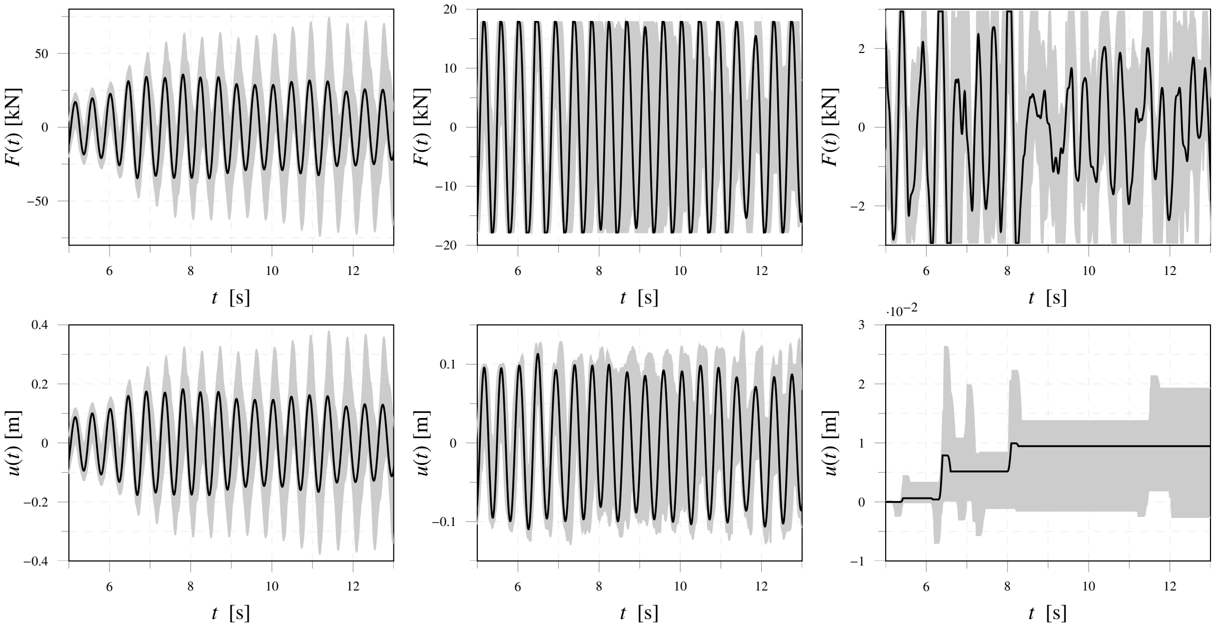

Figure 5: Force (top) and displacement (bottom) time histories a linear (left), elastoplastic (middle) and rigid-plastic (right) secondary system, for Irpinia earthquake, drawn from Gaussian distributions.

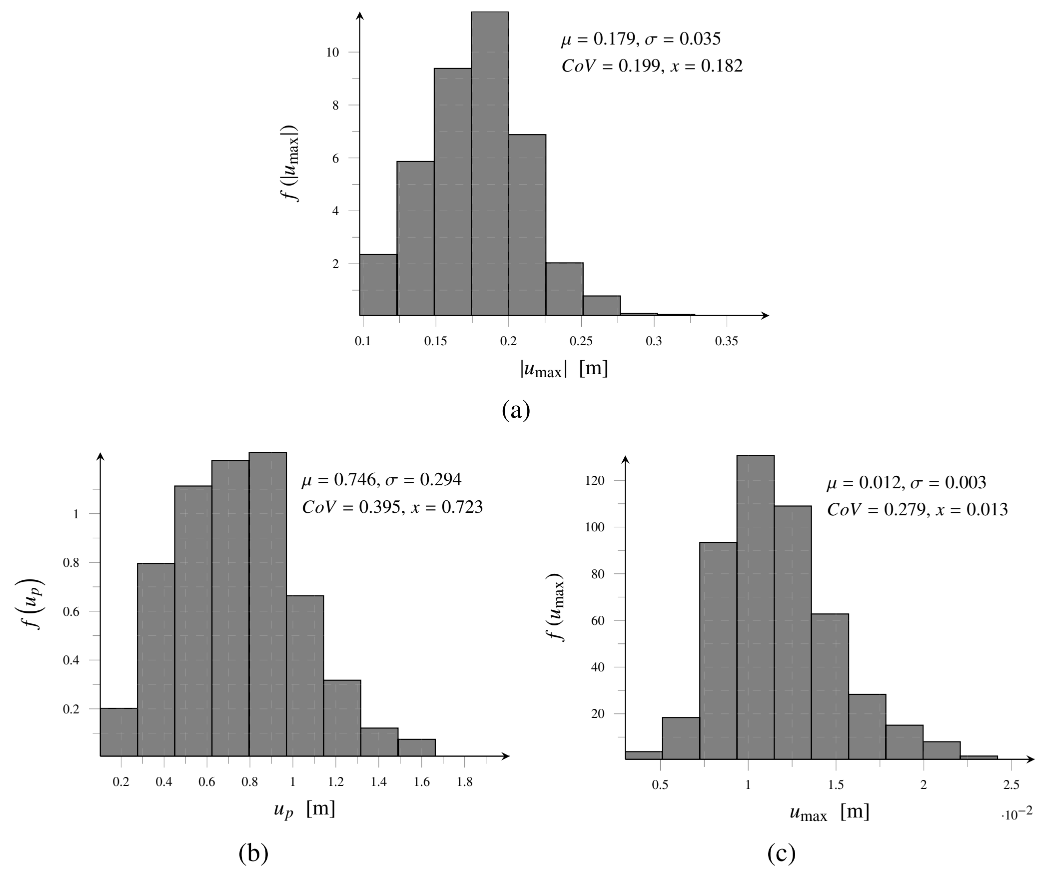

Figure 6: PM frequency diagram for a linear (a) elastoplastic (b) and rigid-plastic (c) secondary system due to Irpinia earthquake, drawn from Gaussian distribution.